Journal of Engineering and Sustainable Development
Vol. 30, No. 04, July 2026
https://jeasd.uomustansiriyah.edu.iq/index.php/jeasd
ISSN 2520-0917
Research Article
https://doi.org/10.31272/jeasd.2701

Comparative Study of the Mechanical and Fatigue Behavior of Aluminum Alloys in Aircraft Fuselages

Zainab H. Lafta[1*], Khuder N. Abed[2], Saad T. Faris[2]

[1]Department of Mechanical Engineering, College of Engineering, University of Diyala, Iraq
[2]Department of Aeronautical Engineering Techniques, Bilad Alrafidain University College, Diyala, Iraq

[*]Email: zainab_hamed@uodiyala.edu.iq

Article Info

Received 19/05/2024
Revised 19/05/2026
Accepted 19/05/2026

Abstract

Aluminum alloys are widely used in aircraft fuselages due to their high strength, light weight, and corrosion resistance. This paper investigates the fatigue and mechanical properties of two aluminum alloys, AA2014 and AA7075-T651, to improve the durability of aircraft fuselages, particularly in high-stress areas such as fuselage joints. Tensile and fatigue tests were conducted according to ASTM E8M-16a and E466 standards in order to determine the properties of the materials in this research. In these tests, the yield (YS), elastic parameter (E), tensile strength (UTS), ductility, and fatigue life were measured under constant and variable load conditions. AA7075-T651 shows a 17% higher yield strength and a 16% higher fatigue strength than AA2014, according to the results. For instance, at 244 MPa, AA7075-T651 endured over 400,000 cycles compared to less than 16,000 cycles for AA2014. The investigation of fatigue crack growth showed that small cracks in AA7075-T651 propagate faster than long cracks due to microstructural interactions. AA7075-T651 exhibited better corrosion resistance than AA2014. These findings indicate that AA7075-T651 is highly suitable for critical, high-pressure aircraft components and contributes to improved safety, longevity, and performance in aerospace applications.

Keywords: Aircraft Fuselage, Aluminum Alloys, Fatigue Life, Mechanical Properties.

1. Introduction

Due to the excellent mechanical properties of Aluminum alloys (strength, weight saving, corrosion resistance), these alloys are used to a large extent in modern aircraft fuselage construction [1]. This has led to increased use of alloys such as AA2014 and AA7075-T651 in this area. In an effort to enhance the performance of these alloys and to make them suitable for critical aerospace applications, advanced processing techniques, such as laser treatments and surface modifications [2] are used. In a study of vibration stress relief, Song and Zhang [3] found that vibration stress can relieve residual stress when the dynamic stress is less than 8% of the yield strength, and that it can extend service life. Besides these treatments, there have been enhancements of the bonding and machining processes for aluminum alloys. Britto and Bino [4] have proposed empirical models for diffusion bonding AA2014 and AA7075 so as to obtain the best possible mechanical properties. Jomaa et al. [5] correlated differences in the performance of high speed machining of AA6061-T6 and AA7075-T651 with differences in the chip formation and residual stress and related it to differences in thermal conductivity and yield strength. Furthermore, Minhas et al. [6] showed that FSW of AA7075-T651 exhibited the finest equiaxed grains and optimum microstructure, which led to maximum hardness. There are also numerous other studies dedicated to fatigue performance and crack growth. Mantha and Fawaz suggested a corrosion pit-to-fatigue crack transition test for testing the prediction of fatigue crack growth in AA7075-T651 material and proposed the test, which was found to be accurate [7]. Zhang et al. [8] used the ultrasonic nanocrystal surface modification (UNSM) process to improve fatigue performance and created favorable compressive residual stresses, increasing surface hardness. The AA7075-T651 was examined under various temperatures and strain rates to investigate its mechanical properties and changes in the microstructure [9]. The key to fatigue life and fracture surface appearance in AA7075-T651 is the use of strain sequences, which highlights the need for the model to be accurate and important, as noted by Macek et al. [10]. Younis et al. [11] used machine learning to enhance the accuracy of the fatigue crack growth rate prediction of aircraft aluminum alloys in the field of predictive modeling. Zhao, and Jiang [12] also

discovered that the mean stress has a strong effect on the fatigue properties of AA7075-T651, both in terms of fatigue strength and crack propagation. With respect to corrosion resistance, Prabhuraj et al. [13] studied it under salt-mist conditions and gave interesting insights into the corrosion behavior of AA7075-T651, which is crucial for aerospace applications. The main concern of this research is the understanding of both fatigue and corrosion behavior of aluminum alloys, especially in critical applications such as parts of aircraft fuselage [14]. In the aircraft industry, the structural integrity of an aircraft's fuselage is a vital consideration, and Chetan et al. [15] have focused on this aspect and estimated the fuselage's fatigue life. Langari et al. [16] explored the fatigue life simulation of AA7075-T651 FSW joints using experimental data as well as by analyzing the joint quality and fatigue behavior. Alssayegh et al. [17] studied the structural strength and the fatigue life of the AA7075-T651 aluminum alloy cleats, and they offered some suggestions for aircraft cleat design. To avoid fatigue failure of critical components like airframes, the multiaxial fatigue behavior of AA7075-T6 samples was investigated by Lay et al. [18] based on acoustic emission analysis.

This paper aims to evaluate and compare the mechanical properties and fatigue behavior of the aluminum alloys AA2014 and AA7075-T651, focusing on their chemical composition, mechanical properties, and fatigue resistance. The purpose of this research is also to study the relationship between applied stress and fatigue life under constant-load conditions, as well as the behavior of crack growth and fatigue performance. The research aims to improve the strength and integrity of these alloys to withstand vibration stress and diffusion bonding by incorporating findings from previous research in both fields.

2. Characterization and Testing of Aluminum Alloys

2.1. Material Choice

Chose AA 7075-T651 and AA2014 as the experimental materials for this study. Aluminum alloys are common choices for fuselage airplane structures due to their lightweight, high strength, and corrosion resistance.

2.1.1. Chemical analyses

The chemical analyses carried out utilizing the Spectro Maxx metal analyzer at the Iraqi Ministry of Industry and Materials under the supervision of the State Company for Inspection and Engineering Qualification (SIER) are noted in Table 1. The table presents the elemental composition of the experimental aluminum alloys AA2014 and AA7075-T651, showing the weight percentages relative to the established standards. Important compositional differences were observed, primarily in silicon (Si), copper (Cu), magnesium (Mg), and zinc (Zn).

Table 1. Chemical analyses of the experimental aluminum alloys AA2014 and AA7075-T651, expressed in weight percent (wt%) and compared with the standard [19].

Element Wt.%	AA7075-T651	AA2014
Si	0.105	0.267
Fe	0.256	0.499
Cu	1.61	4.73
Mn	0.0475	0.412
Mg	2.35	0.521
Cr	0.218	0.0125
Zn	5.67	0.198
Al	Balance	Balance

2.1.2. Mechanical properties

Table 2 presents the mechanical properties of AA2014 and AA7075-T651 alloys under standard and experimental test conditions, including yield strength (YS), elastic modulus (E), ultimate tensile strength (UTS), elongation, and Rockwell hardness (HRB). AA7075-T651 alloy exhibits significantly enhanced properties compared to AA2014 alloy under both conditions.

2.2. Preparation Of Tensile and Fatigue Test Specimens and Test Procedures

In this study, a set of samples was prepared for testing and examination. Ten samples were prepared for fatigue testing, divided into five for AA2014 and five for AA7075-T651, in accordance with ASTM E466. Eight samples were also prepared for tensile testing, with four samples per alloy in accordance with ASTM E8M-16a.

2.2.1. Tensile test

Tensile test specimens were machined in circular form from both alloys (AA2014 and AA7075-T651) in accordance with the ASTM E8M-16a standard to determine their mechanical properties. Then, a tensile force of 600 kN was applied after the specimen was fixed between the handles of a servo-controlled hydraulic tensile testing machine of the United SHFM type, as shown in Fig. 1.

2.2.2. Fatigue test specimen

The dimensions and shapes of the fatigue test specimens, before and after testing, are displayed in Fig. 2 and Fig. 3. All specimens were made in accordance with ASTM E466; all dimensions are given in millimeters (mm).

Table 2. The mechanical properties of AA2014 and AA7075-T651 under test conditions in comparison to the standard test [20].

Alloys	AA2014		AA7075-T651	
Condition	Standard	Experimental	Standard	Experimental
YS (MPa)	424	446	503	590
E (GPa)	75.4	79.5	72.7	77.4
UTS (MPa)	493	534	582	619
Ductility%	12	11.5	11	11
Hardness Rockwell HRB	67	68.4	87	89.12

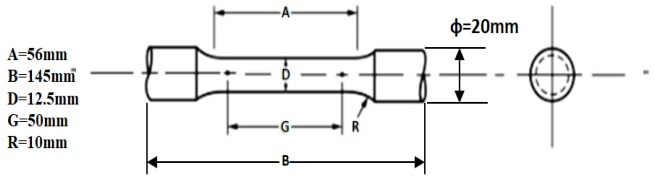

Figure 1. Tensile Test Specimen According to the ASTM E8M-16a Standard.

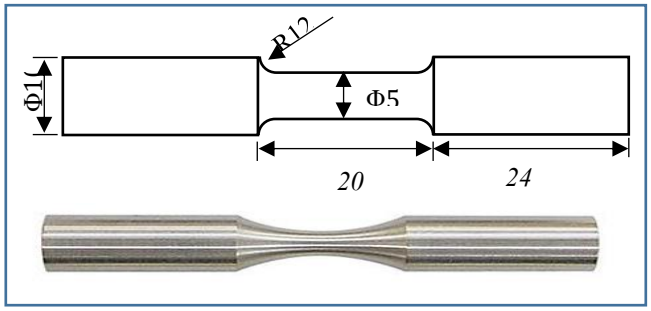

Figure 2. Fatigue Test Specimen According to the ASTM E466 Standard.

Figure 3. Samples of fatigue test specimens, both before and after testing.

2.3. Hardness Test

The hardness of AA2014 and AA7075-T651 aluminum alloys was examined using a Rockwell Tru-Blue Hardness II tester in accordance with the ASTM E18 standard. The tests were conducted at the Iraqi Ministry of Industry and Materials and the State Company for Inspection and Engineering Qualification (SIER). The experimental results of the alloys were later compared with the standard values.

2.4. Crack Length and Growth Rate Measurement

The crack length was measured utilizing the iteration method, where the process starts with cleaning the test place with ultra-pure acetone; later, a cellulose acetate film (15 mm × 10 mm × 0.035 mm) was located on the sample surface, dried, and carefully removed to be located between glass slides for measurement. Employing an optical microscope with a magnification of (400X) to measure the crack length, these measurements were frequently used throughout the fatigue test period. The crack growth rate, also known as the crack velocity, was calculated as the change in crack length per cycle (da/dN) by recording crack lengths across different cycles and determining the growth rate. The optical microscope (400X) provided accurate observations of crack propagation during each iteration. Fig. 4 shows the crack propagation behavior of AA7075-T651 and AA2014 alloys under fatigue loading. The pictures show clear crack paths, revealing the differences in crack growth mechanisms between the two alloys.

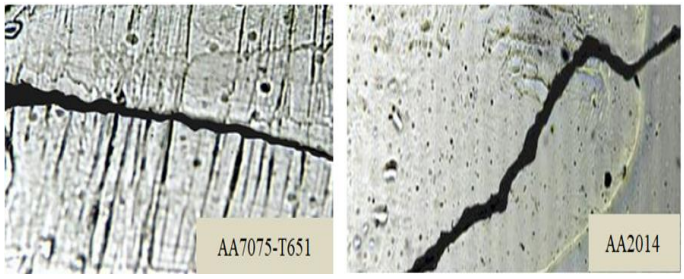

Figure 4. The Cracks of AA7075-T651 and AA2014 alloys.

3. Result

The mechanical properties of experimental and standard aluminum alloys (AA2014 and AA7075-T651) are compared in Table 3 and Fig. 5. AA2014 has superior mechanical properties as compared to the standard alloys. It will have a high YS of 446 MPa, indicating greater resistance to deformation, and an E of 79.5 GPa, indicating greater stiffness. Furthermore, its UTS (ultimate tensile strength) is 534 MPa, exceeding the standard UTS of 493 MPa, indicating it can support a heavy load. However, AA2014 has slightly less ductility and elongation at break of 11.5% against the standard value of 12%, which means it can be stretched less before breaking. In addition, its HRB (Rockwell hardness) is slightly higher at 68.4, which means that it is more resistant to buckling than the typical value.

The experimental AA7075-T651 alloy has better mechanical properties than the standard alloy. The experimental alloy has a significantly higher YS (deformation resistance) of 590 MPa. The elastic modulus (E) is slightly higher, at 77.4 GPa, meaning the experimental alloy is stiffer, but the ultimate tensile strength (UTS) is 619 MPa, which is higher, meaning the experimental alloy is able to withstand a greater load. The ductility of the experimental alloys is comparable to that of the standard alloys, as shown by the elongation at break, which is 11% for both alloys, indicating they can be stretched by a similar amount before breaking. Additionally, the experimental alloy has an increased Rockwell hardness (HRB) of 89.12 as opposed to the standard of 87, which suggests its resistance to scratches and dents.

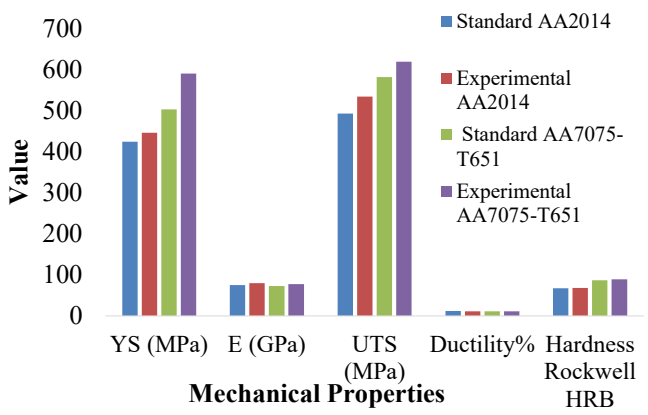

Figure 5. Comparative analysis of mechanical properties between experimental and standard aluminum alloys (AA2014 and AA7075-T651).

Five samples of aluminum alloy (AA2014) were subjected to fatigue testing to determine the S-N curves for these alloys under constant-amplitude loading at RT (room temperature) and an Rs (stress ratio) of -1. The fatigue test data are summarized in Table 3.

This table presents fatigue test results for AA2014 aluminum alloy under constant loading conditions and illustrates the correlation between applied stress (MPa) and the corresponding number of cycles to failure (Nf). As load increases, Nf generally decreases, indicating the typical inverse relationship observed in fatigue testing. For example, when the stress decreases from 324 MPa to 210 MPa, Nf increases from 3567 to 15933 cycles, consistent with the expected behavior of materials under cyclic loading. Fig. 6 shows that the total number of cycles to failure decreases as the load increases.

Table 3. The Fatigue Test Results under Constant Loading of AA2014.

Spec. No.	Applied Stress (MPa)	Nf (cycles)
1	324	3567
2	262	6800
3	244	10133
4	227	13133
5	210	15933

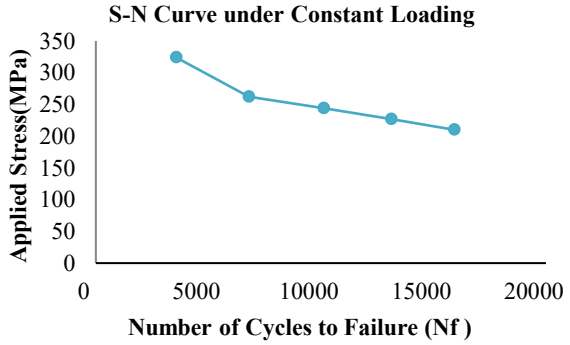

Figure 6. S-N Curve under Constant Loading of AA2014.

Five specimens of aluminum alloy (AA7075-T651) were fatigue tested to analyze the S-N curves (stress-life curves) of this alloy under constant amplitude loading at RT (room temperature) with Rs (stress ratio) = -1. The test results are displayed in Table 4. The table shows the results of fatigue testing performed on five samples of aluminum alloy (AA7075-T651) under a constant load at RT (room temperature) and a stress ratio Rs = -1. Each sample was subjected to a varying load measured in megapascals (MPa), and the corresponding number of failure cycles (Nf) was recorded. The data showed a significant relationship between the applied stress and the fatigue life of the samples. As the load increases, the fatigue life decreases. For example, at the highest applied stress of 366 MPa, the sample endured only 16400 cycles before failure, whereas at the lowest applied stress of 244 MPa, it endured a much longer fatigue life of 412677 cycles. Fig. 7 shows that the total number of failure cycles decreases as the load increases.

Table 4. The Fatigue Test Results under Constant Loading of AA7075-T651.

Spec. No.	Applied Stress (MPa)	Nf (cycles)
1	366	16400
2	315	64433
3	284	190000
4	263	310000
5	244	412677

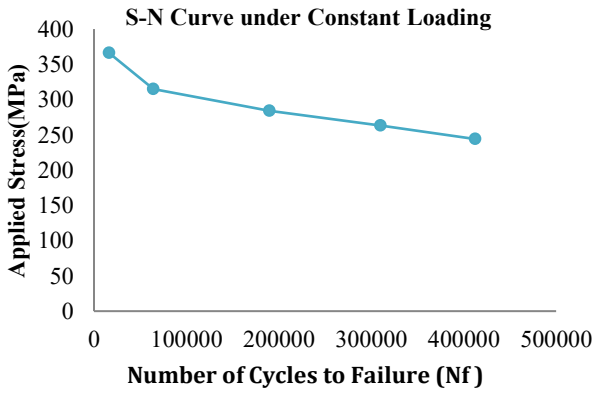

Figure 7. S-N Curve under Constant Loading of AA7075-T651.

For a single fatigue specimen, crack lengths were measured in AA2014 and AA7075-T651 aluminum alloys subjected to stresses of 100 and 120, respectively, under constant-amplitude loading at room temperature with a stress ratio (Rs) of -1. The crack lengths and associated cycle numbers were systematically documented for both alloys until the specimens failed. Fig. 8 and Fig. 9 display the crack growth behavior of AA2014 and AA7075-T651 aluminum alloys and show the correlation between N (cycle number) and initial crack length (a) for every material. The length of the crack was measured employing the repeating method which involved the following procedure: Clean the area of the test with (3-5) drops of ultra-pure acetone and then place 15 mm x 10 mm x 0.035 mm cellulose acetate paper strips on the specimen surface using tweezers. After the leaves have dried for several minutes, the acetate strip is lifted

with forceps and placed between two glass slides. The crack lengths measured by optical microscopy at 400X magnification ranged from 160 µm to 1460 µm over 7000 to 76000 cycles for AA2014 alloys. In the same way, the crack lengths for AA7075-T651 alloys ranged from 120 µm to 1650 µm over 70000 to 885000 cycles. The trend shows a growth in crack length with increasing cycle number, indicating the propagation of fatigue cracks. It is worth noting that the AA2014 alloy generally exhibits shorter crack lengths than AA7075-T651 at similar cycle numbers, suggesting possible different fatigue properties between the two alloys.

Fig. 10 shows the relationship between crack velocity (da/dN in µm/rev) and average crack length (in µm) for AA2014 aluminum alloy under 100 MPa stress. The data show a relationship between crack velocity and average crack length, with significant differences in crack velocity at different average lengths. Generally, cracks with smaller average lengths tend to exhibit faster crack growth rates, while cracks with larger average lengths are related to slower crack growth rates. This shows that the size of existing cracks significantly affects crack growth behavior in AA2014, with small cracks propagating faster than large ones.

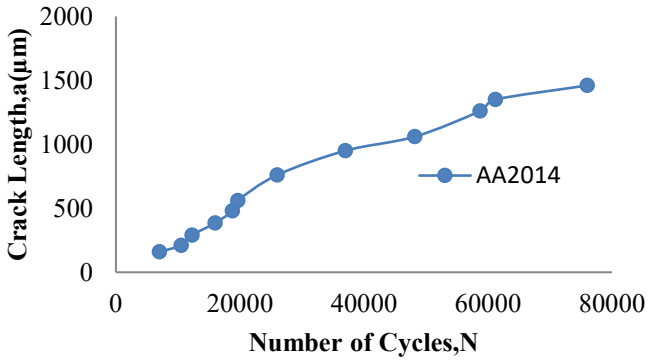

Figure 8. The crack growth behavior for AA2014.

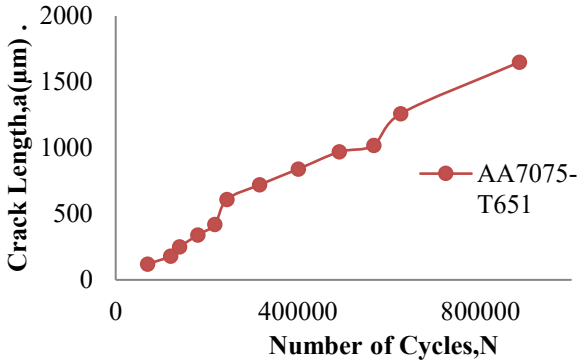

Figure 9. Crack growth behavior of AA7075-T651 aluminum alloy.

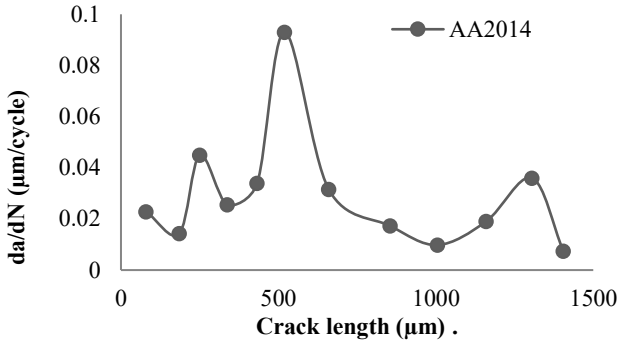

Figure 10. Crack velocity rate (da/dN in µm/cycle) and average crack length (in µm) data for AA2014 aluminum alloy.

Fig. 11 shows the average crack velocity (da/dN, in µm/rev) and the corresponding average crack length (a, in µm) for AA7075-T651 aluminum alloy under a constant stress of 120 MPa. The data show a nonlinear relationship between the crack velocity and the average crack length. When the crack length increases from 60 µm to 295 µm, the average crack velocity changes irregularly at first, but beyond 295 µm, a noticeable increase in crack velocity with average crack length becomes apparent. On the other hand, there are deviations from this behavior at some specific crack lengths, such as 515 µm and 1140 µm (which indicates that other factors may be affecting the crack propagation behavior, such as the microscopic properties of the materials or residual stress interactions.

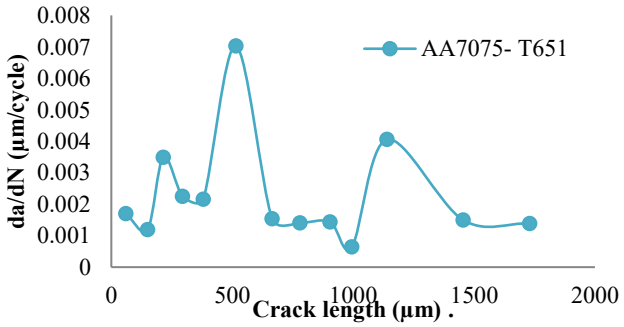

Figure 11. shows crack velocity rate data (da/dN, in µm/cycle) and the corresponding average crack length (in µm) for aluminum alloy AA7075-T651.

Fig. 12 shows the difference in the mechanical properties of the aluminum alloys AA2014 and AA7075-T651 under tensile loading, as shown in the stress-strain curves. At 1.1% strain, the maximum stress value of 619 MPa is achieved by alloy AA7075-T651. This indicates its superior strength and high resistance to deformation. However, the AA2014 alloy reaches a maximum stress of 534 MPa at 1.2% strain, indicating good mechanical properties but lower strength than AA7075-T651. Based on the information provided, it is clear that applications requiring high strength and resistance to deformation are better suited to the AA7075-T651 alloy. However, there are several

structural applications where AA2014 is useful but may be less suitable under high-stress conditions.

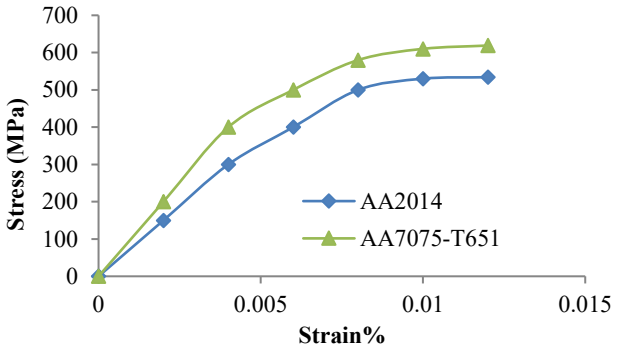

Figure 12. Stress-Strain Curves for AA2014 and AA7075-T651 alloys.

4. Conclusions

In the test results, compared with standard alloys, aluminum alloy (AA7075-T651) showed a 17% increase in yield strength and a 6% increase in ultimate tensile strength. In contrast, aluminum alloy AA2014 showed significant improvement up to 5. % Increase in yield strength and ultimate tensile strength. AA2014 showed a significant improvement of up to 5% in yield strength and an 8 % increase in ultimate tensile strength, indicating a significant improvement in its mechanical properties. Regarding the stress-strain curves of both alloys, the analysis highlights differences in their behavior under tensile loading. The results for aluminum alloy AA7075-T651 showed that the stress reached a maximum of 619 MPa at 1.1% strain, indicating high strength and deformation resistance. AA2014, however, achieved a maximum stress of 534 MPa at 1.2% strain and had good mechanical properties with low strength, thus not suitable for use in conditions that need to resist high strains. In addition, AA7075-T651 had outstanding fatigue properties and was able to withstand a long duration of constant loading. It was noted that the AA7075-T651 alloy endured over [412,000 cycles], whereas the AA2014 alloy only had a fatigue life of less than [16000 cycles] due to its lower fatigue resistance compared to the AA7075-T651 alloy. The crack growth test on both alloys also revealed that the AA2014 alloy possessed the lower crack growth length, indicating slightly higher crack growth resistance in the initial stages of the test compared to the AA7075-T651 alloy. But the fatigue strength of AA7075-T651 overall is greater. The results also showed non-linear crack growth behavior, indicating the influence of several factors, such as stress interactions and the material's internal structure.

Conflict of interest

The authors declare that there are no conflicts of interest regarding the publication of this manuscript.

Author Contribution Statement

Zainab H. Lafta and Khuder N. Abed conducted sample testing and discussed the results.

Saad T. Faris proposed the problem under investigation and supervised the results.

References

[1] B. Malek, C. Mabru, and M. Chaussumier, "Fatigue behavior of 2618-T851 aluminum alloy under uniaxial and multiaxial loadings," *International Journal of Fatigue*, vol. 131, no. 105322, Feb. 2020. doi: https://doi.org/10.1016/j.ijfatigue.2019.105322.

[2] S.-S. Li, X. Yue, Q.-Y. Li, H.-L. Peng, B.-X. Dong, T.-S. Liu, H.-Y. Yang, J. Fan, S.-L. Shu, F. Qiu, and Q.-C. Jiang, "Development and applications of aluminum alloys for aerospace industry," *Journal of Materials Research and Technology*, vol. 27, pp. 944–983, Nov.–Dec. 2023, doi: https://doi.org/10.1016/j.jmrt.2023.09.274

[3] J. Song and Y. Zhang, "Effect of vibratory stress relief on fatigue life of aluminum alloy 7075-T651," *Advances in Mechanical Engineering*, vol. 8, no. 6, no. 1687814016654379, 2016. doi: https://doi.org/10.1177/1687814016654379.

[4] A. S. F. Britto and J. S. Binoj, "Mechanical properties optimization and microstructures of diffusion bonded AA2014/AA7075 Al alloys," *Revista de Metalurgia*, vol. 58, no. 3, no. e225, 2022. doi: https://doi.org/10.3989/revmetalm.225.

[5] W. Jomaa, S. Lavernhe, E. Duc, and P. Ray, "FEA-based comparative investigation on high-speed machining of aluminum alloys AA6061-T6 and AA7075-T651," *Solid State Phenomena*, vol. 261, pp. 347–353, 2017. doi: https://doi.org/10.4028/www.scientific.net/SSP.261.347.

[6] N. Minhas, V. Sharma, S. Manda, and A. Thakur, "Insights into the microstructure evolution and mechanical behavior of dissimilar friction stir welded joints of additively manufactured AlSi10Mg and conventional 7075-T651 aluminum alloys," *Materials Science and Engineering: A,* vol. 881, no. 145407, Aug. 2023, doi: https://doi.org/10.1016/j.msea.2023.145407

[7] D. Mantha, M. J. Hammond, and S. Fawaz, "Corrosion pit to fatigue crack transition methodology for AA7075-T651 aluminum alloy," in *Proc. 2013 DoD Corrosion Conference*, 2013. [Online]. Available: https://apps.dtic.mil/sti/citations/AD1042267.

[8] R. Zhang, R. Chiang, Z. Ren, H. Zhang, W. Zhao, G.-X. Wang, V. K. Vasudevan, Y. Dong, and C. Ye, "Fatigue performance improvement of 7075-T651 aluminum alloy by ultrasonic nanocrystal surface modification," *Journal of Materials Engineering and Performance*, vol. 31, pp. 2354–2363, Mar. 2022. doi: https://doi.org/10.1007/s11665-021-06308-9.

[9] B. Dalai, "Material Characterization of AA7075-T651 Deformed at Different Temperatures and Strain Rates," Ph.D. dissertation, Luleå University of Technology, 2021.

[10] W. Macek, R. Branco, J. D. Costa, and C. Pereira, "Strain sequence effect on fatigue life and fracture surface topography of 7075-T651 aluminium alloy," *Mechanics of Materials*, vol. 160, no. 103972, Sep. 2021. doi: https://doi.org/10.1016/j.mechmat.2021.103972.

[11] H. B. Younis, K. Kamal, M. F. Sheikh, and A. Hamza, "Prediction of fatigue crack growth rate in aircraft aluminum alloys using optimized neural networks," *Theoretical and Applied Fracture Mechanics*, vol. 117, no. 103196, Feb. 2022. doi: https://doi.org/10.1016/j.tafmec.2021.103196.

[12] T. Zhao and Y. Jiang, "Fatigue of 7075-T651 aluminum alloy," *International Journal of Fatigue*, vol. 30, no. 5, pp. 834–849, 2008. doi: https://doi.org/10.1016/j.ijfatigue.2007.07.005

[13] P. Prabhuraj, S. Rajakumar, and V. Balasubramanian, "Developing empirical relationship to predict corrosion rate of high strength AA 7075-T651 aluminium alloy under salt fog environment," *International Journal of Electroactive Materials*, vol. 4, pp. 44–49, 2016. [Online]. Available: https://www.electroactmater.com/IJEM/4-4-44-49.pdf?utm.

[14] P. Parasuraman, S. Rajakumar, M. Ramachandran, and V. Balasubramanian, "Stir zone stress corrosion cracking behavior of friction stir welded AA7075-T651 aluminum alloy joints," *Corrosion Reviews*, vol. 39, no. 1, pp. 55–62, 2021. doi: https://doi.org/10.1515/corrrev-2020-0065.

[15] B. S. Chetan, G. N. Swamy, and K. E. Girish, "Fatigue life estimation of rear fuselage structure of an aircraft," *International Journal of Research in*

Engineering and Technology, vol. 4, no. 7, pp. 347–354, Jul. 2015. doi: https://doi.org/10.15623/ijret.2015.0407056.

[16] J. Langari, K. Aliakbari, and F. Kolahan, "Fatigue life simulation of AA7075-T651 FSW joints using experimental data," *Engineering Failure Analysis,* vol. 154, p. 107690, 2023. doi: https://doi.org/10.1016/j.engfailanal.2023.107690

[17] D. Tong, B. Hu, B. Chen, J. Li, J. Di, H. Wang, S. Zhou, and W. Yang, "Analysis of structural strength and fatigue life based on the 7075-T651 aluminum alloy lugs," *Journal of Physics: Conference Series*, vol. 2679, no. 1, no. 012003, 2024. doi: https://doi.org/10.1088/1742-6596/2679/1/012003.

[18] A. Alssayegh, M. Y. Abdellah, M. K. Hassan, S. Azam, A. Melaibari, and U. A. Khashaba, "Optimizing high cycle fatigue predictions in notched Al 7075-T6: An analytical approach to rotating bending behavior," *Results in Engineering*, vol. 25, Art. no. 103623, Mar. 2025, doi: https://doi.org/10.1016/j.rineng.2024.103623.

[19] ASTM International, "ASTM E112-13(2021) Standard Test Methods for Determining Average Grain Size," ASTM International, 2021. Accessed: Jun. 22, 2024. [Online]. Available: https://www.astm.org/e0112-13r21.html.

[20] ASTM International, "ASTM B211-12(2021) Standard Specification for Aluminum and Aluminum-Alloy Rolled or Cold Finished Bar, Rod, and Wire," ASTM International, 2021. Accessed: Jun. 22, 2024. [Online]. Available: https://webstore.ansi.org/standards/astm/astmb21112e1